Excitonic Aharonov-Bohm effect in a two-dimensional quantum ring

C. González-Santander,[1,*] F. Domínguez-Adame,[1] and R. A. Römer[2]

[1]*Departamento de Física de Materiales, Universidad Complutense de Madrid, ES-28040, Spain*

[2]*Department of Physics and Centre for Scientific Computing, University of Warwick, Coventry, CV4 7AL, United Kingdom*

(Received 13 July 2011; published 1 December 2011)

We study theoretically the optical properties of an exciton in a two-dimensional ring threaded by a magnetic flux. We model the quantum ring by a confining potential that can be continuously tuned from strictly one-dimensional to truly two-dimensional with finite radius-to-width ratio. We present an analytic solution of the problem when the electron-hole interaction is short ranged. The oscillatory dependence of the oscillator strength as a function of the magnetic flux is attributed to the Aharonov-Bohm effect. The amplitude of the oscillations changes upon increasing the width of the quantum ring. We find that the Aharonov-Bohm oscillations of the ground state of the exciton decrease with increasing the width, but, remarkably, the amplitude remains finite down to radius-to-width ratios less than unity. We attribute this resilience of the excitonic oscillations to the nonsimple connectedness of our chosen confinement potential with its centrifugal core at the origin.

DOI: 10.1103/PhysRevB.84.235103 PACS number(s): 71.35.Cc, 03.65.Ge

I. INTRODUCTION

Recent advances in nanofabrication of quantum rings and dots by self-assembling,[1–5] lithographic,[6,7] or etching techniques[8] have opened an active area of research both theoretical and experimental. In such systems, electrons and holes are confined in a small region and consequently the Coulomb interaction is enhanced. The existence of bound states of electron-hole pairs offers a unique opportunity to explore the Aharonov-Bohm (AB) effect[9–12] for excitons in quantum rings.[13,14] Despite the exciton being a neutral entity, it has been predicted to be sensitive to a magnetic flux due to its finite size inside a quantum ring.[13,14] In experiments, this sensitivity would show as an oscillatory dependence of both the optical transition energy as well as the oscillator strength upon the magnetic flux.[4,7,8,15–17] Theoretically, the excitonic AB effect has been studied by a variety of different approaches. A short-range interaction between the electron and the hole has been investigated for one-dimensional (1D) rings,[13,14,18,19] where also the effect of an external electric field can be included.[20] Intermediate models assume two-dimensional (2D) rings with narrow width under harmonic confinement and Coulomb-like interaction potentials between the electron and the hole,[21,22] or radial-polarized excitons when electrons and holes move in different circles.[23–25] The excitonic AB effect in 2D rings has been studied in models with harmonic[26] and geometric[15,27,28] confining potential or using a 2D attractive annular Hubbard model.[29,30] In all cases, the excitonic AB effect for neutral excitons has been argued to be suppressed in 2D as the width of the ring is increased.[31] Recently, experimental results in molecular-beam-epitaxy grown nanorings made by $AsBr_3$[8] etching and on self-assembled InAs/GaAs quantum dots[5] report oscillations in the binding energy of neutral excitons that may be accounted for by the excitonic AB effect.

In this paper, we consider the excitonic AB effect in a confining potential that can be continuously tuned from strictly 1D to truly 2D with finite radius-to-width ratio while preserving the central structure of a ring, namely, its nonsimple connectedness due to an infinitely strong repulsion at the origin.[32] We present a simple analytic approach to the excitonic problem when the electron-hole attraction is short ranged.[13,14] We then study how the amplitude of the AB oscillations in the oscillator strength changes upon increasing the width of the ring. We find that the AB oscillations of the exciton ground-state energy decrease with increasing width of the quantum ring, but, nevertheless, the effect remains noticeable down to regimes with radius-to-width ratios smaller than unity. This shows the robustness of the excitonic AB effect in 2D.

II. SINGLE-PARTICLE STATES IN THE QUANTUM RING

In the absence of Coulomb interaction, the Hamiltonian of a single particle (electron or hole) subjected to a magnetic flux in a 2D quantum ring is given by

$$\mathcal{H}_i = \frac{1}{2m_i}(\boldsymbol{p}_i - q_i \boldsymbol{A})^2 + V(r_i), \tag{1}$$

where m_i, $\boldsymbol{p}_i$, and $\boldsymbol{A}$ are the effective mass, the momentum in the plane, and magnetic vector potential, respectively. Here, the subscript $i = e,h$ refers to the electron and the hole, respectively. Electric charges are $q_e = -e$ and $q_h = e$. The quantum ring is modeled by an anharmonic, axially symmetric potential with a centrifugal core[32,33]

$$V(r_i) = \frac{V_0}{2}\left[\frac{R^2}{r_i^2} + \frac{r_i^2}{R^2}\right] - V_0. \tag{2}$$

The confining potential has the minimum at $|\boldsymbol{r}_i| = R$ (see Fig. 1) and, for this reason, R will be used as a convenient measure of the effective ring radius. Close to the minimum, the potential reduces to the well-known displaced parabola, $V(r_i) = 2V_0(r_i/R - 1)^2 \equiv (1/2)m_i\omega^2(r_i - R)^2$, used in other theoretical studies of 2D quantum rings.[26] As $r_i \to 0$, we see from Eq. (2) that the centrifugal core assures the survival of the essential feature of a ring: its repulsive barrier in the center. The effective width W of the quantum ring can be estimated from the single-particle ground state in the harmonic potential, namely, $W = (\epsilon_0/2V_0)^{1/4}R$, where $\epsilon_0 = \hbar^2/2mR^2$ is the ring-size quantization energy.[32] Notice that we assume that W is the same for electrons and holes, namely, $m_e = m_h \equiv m$. For the purpose of this work, all energies will be measured in units of

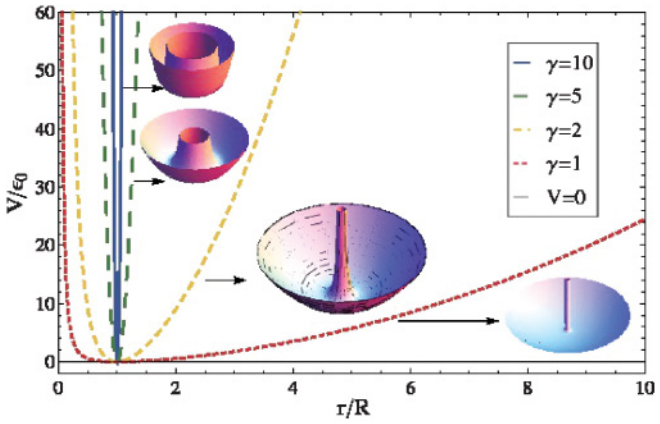

FIG. 1. (Color online) Plot of the radial dependence of the confining potential for $\gamma = 1$ (short-dashed), 2 (dashed), 5 (long-dashed), and 10 (solid). The strongly repulsive core at the origin remains very prominent even for decreasing γ.

ϵ_0 and we parametrize the strength of the confining potential by the radius-to-width ratio $\gamma \equiv R/W = (2V_0/\epsilon_0)^{1/4}$. When $\gamma \to \infty$, we approach the limit of a 1D ring, whereas $\gamma \to 0$ corresponds to an antidot geometry.[32] Figure 1 shows the radial confining potential for different values of γ.

In order to study the AB effect in the quantum ring, we choose $\boldsymbol{A} \equiv (A_r, A_\theta) = (0, \Phi\, h/e2\pi r)$, corresponding to an infinitely thin magnetic flux piercing the plane of the ring perpendicularly. Here, Φ is the dimensionless flux through the ring and h/e is the universal flux quantum.[34] We note that due to the axial symmetry around the ring axis, all our results for energies have to be periodic in Φ with period 1, and we hence restrict ourselves to the sector $\Phi \in [0,1]$. Then the Schrödinger equation for the electron in polar coordinates $\boldsymbol{r}_e = (r_e, \theta_e)$ is written in dimensionless form:

$$\mathcal{H}_e \psi_{M_e}(\boldsymbol{r}_e) = \lambda_{M_e} \psi_{M_e}(\boldsymbol{r}_e) = \left[-\frac{\partial^2}{\partial \rho_e^2} - \frac{1}{\rho_e}\frac{\partial}{\partial \rho_e} - \frac{1}{\rho_e^2}\frac{\partial^2}{\partial \theta_e^2} - \frac{2i\Phi}{\rho_e^2}\frac{\partial}{\partial \theta_e} + \frac{\Phi^2}{\rho_e^2} + \frac{V_e}{\epsilon_0} \right] \psi_{M_e}(\boldsymbol{r}_e), \quad (3)$$

where $M_e = (n_e, \ell_e)$ represents the set of quantum numbers for the electron, which are $n_e = 0,1,2,\ldots$ and $\ell_e = 0, \pm 1, \pm 2, \ldots$. For brevity, we define the dimensionless energy $\lambda_{M_e} = E_{M_e}/\epsilon_0$ and radial coordinate $\rho_e = r_e/R$. The Schrödinger equation for the hole is the same aside from a change in sign in the linear term on Φ, and with a set of quantum numbers $M_h = (n_h, \ell_h)$.

The normalized eigenfunctions of Eq. (3) are given by[32]

$$\psi_{M_e}(\boldsymbol{r}_e) = \frac{e^{-i\ell_e\theta_e}}{\sqrt{2\pi}} \mathcal{R}_{M_e}(r_e), \quad (4a)$$

$$\mathcal{R}_{M_e}(r_e) = \frac{1}{R}\left[\frac{\Gamma(n_e+1)}{2^{k_e}\Gamma(n_e+k_e+1)}\right]^{1/2} \times (\rho_e\gamma)^{k_e} e^{-\rho_e^2\gamma^2/4} L_{n_e}^{k_e}\left(\frac{\rho_e^2\gamma^2}{2}\right), \quad (4b)$$

where $k_e = \sqrt{f_e^2 + \gamma^4/4}$ with $f_e = \ell_e - \Phi$ defining an effective angular quantum number due to the confinement and the magnetic flux. L_n^k stands for the generalized Laguerre polynomials. The corresponding dimensionless energies are $\lambda_{M_e} = \gamma^2(2n_e + 1 + k_e) - \gamma^4/2$. The eigenfunctions and energies for the hole are the same as for the electron, with an effective angular quantum number $f_h = \ell_h + \Phi$. The dimensionless zero-point energy ($n_e = \ell_e = \Phi = 0$) for the electron is $\lambda_e^0 = \gamma^2$.

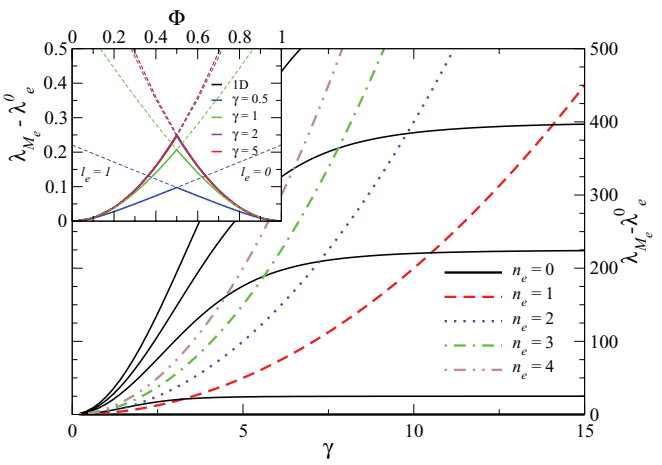

FIG. 2. (Color online) Dimensionless electron energy λ_{M_e} as a function of the radius-to-width ratio γ. Solid, dashed, dotted, dotted-dashed, and double-dotted-dashed lines corresponds to $n_e = 0,1,2,3,4$ and $l_e = 0$. For $n_e = 0$, we also show $l_e = 5,10,15,20$. The flux is $\Phi = 0$ in all cases. The inset shows the flux dependence of the energy of the ground state for different γ. The black lines corresponds to 1D results.

Figure 2 shows the electron energy as a function of the parameter γ. We note that levels at higher values of the quantum number n_e become increasingly uncoupled for $\gamma > 5$ and hence we expect to see nearly 1D behavior for γ values beyond this regime.[14] From the inset, it is clearly observed that in this 2D confinement regime, in the absence of interaction, the ground-state energy for the electron (once the zero-point energy is subtracted) describes an oscillation with the magnetic flux. For $\gamma > 5$, the 2D oscillation is indistinguishable from the 1D case.

III. SOLUTION OF THE EXCITONIC CASE

Within the effective-mass approximation, the Hamiltonian of the interacting electron-hole pair is given by $\mathcal{H} = \mathcal{H}_e + \mathcal{H}_h + \mathcal{H}_{e\text{-}h}$, where $\mathcal{H}_{e\text{-}h}$ is the interaction term. We model the excitonic interaction between the electron and the hole as a short-range potential of the form $\mathcal{H}_{e\text{-}h}(\boldsymbol{r}_e, \boldsymbol{r}_h)/\epsilon_0 = (2\pi)^{3/2} v_0 RW \delta(\boldsymbol{r}_e - \boldsymbol{r}_h)$, where $v_0 < 0$ parametrizes the attractive interaction strength. This contact interaction is the same used in Refs. 14 and 20 extended to a 2D case, where the area of the ring is $2\pi RW$. In this definition, we have carefully chosen the prefactors such that in the 1D limit, $\gamma \to \infty$, the values of v_0 become identical to the corresponding 1D parameter and facilitate comparison with the results of Refs. 14 and 20. Thus, we express v_0 as $-\alpha/\pi^2$, where α denotes the ratio of 1D excitonic Bohr radius to ring circumference.[14]

Before continuing with the detailed study of the model, let us discuss some of the assumptions made and the limitations

that we will encounter. Let us first emphasize that the restriction to equal electron and hole masses is simply a presentational convenience; all calculations shown here can easily be generalized to the case of unequal masses,[20] but with a certain loss of clarity in the mathematical expressions. Nevertheless, we shall present some results for unequal masses later. The assumption of an infinitely thin current-carrying solenoid generating the magnetic flux Φ is a theoretical construct. The experiments cited in the introduction all use a magnetic field B to generate the required Φ. This results in an additional, diamagnetic term proportional to B^2, which we ignore here similarly to the experimental papers.[4,7,8,15–17] Certainly, the most drastic assumption seems to be the δ-function potential for the two-particle interaction. Its use is of course motivated by our resulting ability to reduce the computational difficulties as we will show below. Nevertheless, we wish to emphasize that there are also certain conceptual advantages associated with it: (i) in 1D, the δ function interacting many-particle problem has been solved exactly and hence the expression for the exciton binding energy on a line is known in terms of v_0.[35] (ii) In Ref. 14, it was shown how the Bohr radius of the exciton similarly depends on v_0. Both these parameters will of course vary when another form of interaction is considered. However, as also shown in Ref. 14, it is the ratio α introduced above that governs the strength of the AB oscillations. The effect of other two-particle interaction potentials along the ring, when expressed in terms of α, will lead to similar AB oscillations and we expect at least qualitative agreement. Even for a long-range potential such as the Coulomb interaction, we expect this to hold as long as the overlap of wave packets on opposite sides of the ring, i.e., across the origin at $\boldsymbol{r} = 0$, can be neglected. For the confining potential considered here, with its strong centrifugal core, this should be a rather good approximation.

We construct the exciton eigenfunction as a linear combination of the electron and hole single-particle eigenfunctions:

$$\Psi(\boldsymbol{r}_e,\boldsymbol{r}_h) = \sum_{M_e M_h} A_{M_e M_h} \psi_{M_e}(\boldsymbol{r}_e)\psi_{M_h}(\boldsymbol{r}_h). \tag{5}$$

The Schrödinger equation for the electron-hole pair may now be cast in equivalent form:

$$\sum_{M_e M_h} A_{M_e M_h}(\lambda_{M_e} + \lambda_{M_h} - \Delta)\psi_{M_e}(\boldsymbol{r}_e)\psi_{M_h}(\boldsymbol{r}_h) + (2\pi)^{3/2} v_0 R W \delta(\boldsymbol{r}_e - \boldsymbol{r}_h)\Psi(\boldsymbol{r}_e,\boldsymbol{r}_h) = 0, \tag{6}$$

where Δ is the excitonic energy in units of ϵ_0. Following an analogous procedure as in Ref. 20, the coefficients $A_{M_e M_h}$ are obtained by multiplying Eq. (6) by $\psi^\dagger_{M_e}(\boldsymbol{r}_e)\psi^\dagger_{M_h}(\boldsymbol{r}_h)$ and integrating over the coordinates:

$$A_{M_e M_h} = -\frac{(2\pi)^{3/2} v_0 R W}{\lambda_{M_e} + \lambda_{M_h} - \Delta} G_{M_e M_h}, \tag{7}$$

where we have defined

$$G_{M_e M_h} = \int d^2\boldsymbol{r}\, \Psi(\boldsymbol{r},\boldsymbol{r})\, \psi^\dagger_{M_e}(\boldsymbol{r})\psi^\dagger_{M_h}(\boldsymbol{r}). \tag{8}$$

Setting $\boldsymbol{r}_e = \boldsymbol{r}_h = \boldsymbol{r}$ in the expansion of Eq. (5), multiplying by $\psi^\dagger_{M'_e}(\boldsymbol{r})\psi^\dagger_{M'_h}(\boldsymbol{r})$ and integrating over the coordinates, we finally obtain

$$G_{M'_e M'_h} = \sum_{M_e M_h} G_{M_e M_h} P_{M_e M_h M'_e M'_h}(\Delta), \tag{9}$$

with

$$P_{M_e M_h M'_e M'_h} = -\frac{(2\pi)^{3/2} v_0 R W}{\lambda_{M_e} + \lambda_{M_h} - \Delta} \times \int d^2\boldsymbol{r}\, \psi_{M_e}(\boldsymbol{r})\psi_{M_h}(\boldsymbol{r})\psi^\dagger_{M'_e}(\boldsymbol{r})\, \psi^\dagger_{M'_h}(\boldsymbol{r}). \tag{10}$$

To proceed, we define the total angular momentum of the electron-hole pair in units of $\hbar$ as $L = \ell_e + \ell_h$. Because the system is axially symmetric, only states with $L = L'$ can contribute to the excitonic system. This condition is even more restrictive under the dipole approximation, i.e., only excitons with total angular momentum $L = 0$ can absorb light polarized perpendicular to the ring. Therefore Eq. (10) reduces to

$$P_{M_e M_h M'_e M'_h} = -\frac{\sqrt{2\pi}\, v_0 R W}{\lambda_{M_e} + \lambda_{M_h} - \Delta} \times \int_0^\infty dr\, r\, \mathcal{R}_{M_e}(r)\mathcal{R}_{M_h}(r)\mathcal{R}_{M'_e}(r)\mathcal{R}_{M'_h}(r). \tag{11}$$

We note that in the limit $\gamma \to \infty$, the integrals in Eq. (11) reduce to $1/\sqrt{2\pi} RW$ for $n_e = n_h = n'_e = n'_h = 0$ and $l_e + l_h = l'_e + l'_h$. For other combinations of n_e, n_h, n'_e, and n'_h, the corresponding $P_{M_e M_h M'_e M'_h}$ are less important due to the energy denominator in Eq. (11).

Similarly as for 1D quantum rings,[14,20] there is no analytical solution of Eq. (9) for finite values of v_0. In order to find approximate solutions, we hence need to cut off the sums at some maximally allowed values for M_e and M_h. Figure 2 shows that for smaller values of γ, i.e., increasing ring width W, the level separation between the quantum states of the single particles is decreased. Therefore we use different $\ell_{\max}$ and $n_{\max}$ values depending on our choice of γ. We have tested that our results do not change appreciably for the range of Φ and v_0 considered here. As in Ref. 20, Eq. (9) is reformulated as a standard left-eigenvalue equation $G_{K'} = \sum_K G_K P_{KK'}(\Delta)$ after mapping the quantum numbers $M_e, M_h \to K$ and $M'_e, M'_h \to K'$ according to $K = (\ell + \ell_{\max})(n_{\max}+1)^2 + n_e(n_{\max}+1) + n_h + 1$ such that $K, K' = 1,2,\ldots,(1+2\ell_{\max})(1+n_{\max})^2$. The excitonic energies are obtained numerically by determining the values of Δ that result in the matrix $P_{KK'}$ having an eigenvalue equal to 1. For a given Δ, all eigenstates can be found using Eqs. (9), (7), and (5). An advantage of our approach is that it allows us to target the ground state directly by choosing a suitable starting value for Δ.

IV. RESULTS

In Fig. 3, we plot the ground-state energy Δ defined by Eq. (9) with $\ell_{\max} = 40$ for $\gamma > 0.5$ and $n_{\max} = 5$ ($K_{\max} = 2916$) for $\gamma < 5$ or $n_{\max} = 2$ ($K_{\max} = 729$) for $\gamma > 5$ and as a function of v_0 for different values of γ. For $\gamma = 0.5$ we have used $\ell_{\max} = 30$ and $n_{\max} = 6$ ($K_{\max} = 2989$). Here and in all

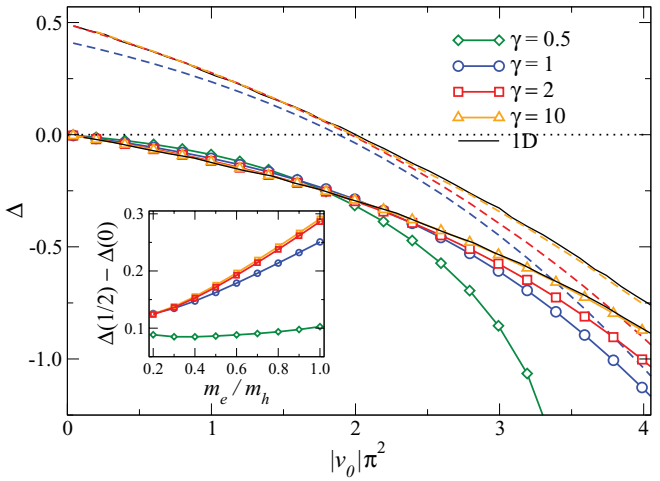

FIG. 3. (Color online) Exciton energy Δ at magnetic flux $\Phi = 0$ (solid lines) and $1/2$ (dashed lines) plotted as a function of the interaction strength v_0. For clarity, symbols are shown for $\Phi = 0$ only and the results for $\gamma = 0.5$ at $\Phi = 1/2$ have been suppressed. The thin dotted horizontal line denotes the onset of the single-particle continuum at $\Phi = 0$. The two thin black lines denote the 1D limit for $\Phi = 0, 1/2$. The inset shows the amplitude of the excitonic AB oscillations as a function of the ratio m_e/m_h at interaction strength $v_0 = -2/\pi^2$.

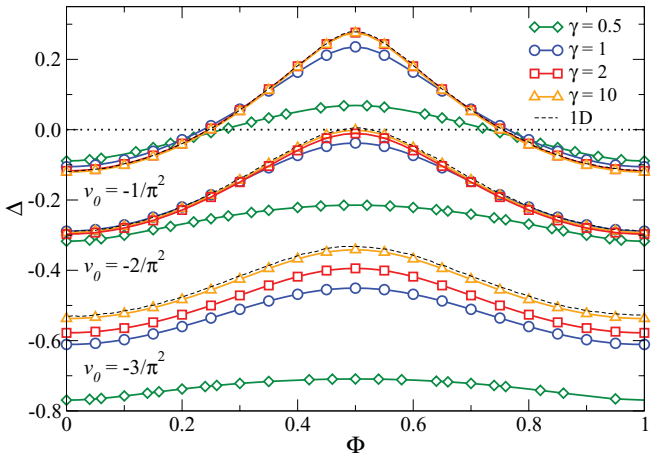

FIG. 4. (Color online) Exciton energy Δ as a function of the magnetic flux Φ for different values of interaction strength v_0 and radius-to-width ratio γ. The thin dotted horizontal line denotes the onset of the single-particle continuum at $\Phi = 0$. Only every second data point is shown for clarity in each curve.

following figures, when plotting the excitonic energies Δ, we have subtracted the zero-point energy $2\gamma^2$ of the noninteracting electron-hole system.

We see that for all γ and Φ values, the increase of the interaction strength v_0 leads to the formation of a state with decreasing energy values below the onset of the free-particle continuum. We also compare in Fig. 3 the 2D exciton results with the 1D ring studied in Refs. 14 and 20. When the radius of the ring is 10 times its width ($\gamma = 10$) the 2D excitonic behavior is essentially indistinguishable from the 1D results in the range of v_0 values studied. In particular, the differences between energies at different flux values at large γ decrease. Nevertheless, for small $\gamma \lesssim 3$, different magnetic flux values lead to quite distinct Δ values—even in a 2D quantum ring the exciton is sensitive to the magnetic flux. It is also interesting to note that for large γ, the bound-state energies are more negative for larger values of v_0 (see Ref. 14), whereas for $\gamma \lesssim 1$, we find evidence that smaller γ values lead to smaller differences between different values of Φ.

The above results have been obtained assuming the same effective mass for the electron and the hole. To address the question of the robustness of the excitonic AB effect in a more realistic situation with different effective electron and hole masses, we have calculated the exciton energy as a function of the ratio m_e/m_h. Let us define the amplitude of the excitonic AB oscillations as the difference of the exciton energy at $\Phi = 1/2$ and $\Phi = 0$, namely $\Delta(1/2) - \Delta(0)$. The inset of Fig. 3 shows this amplitude as a function of the ratio m_e/m_h for different values of γ at interaction strength $v_0 = -2/\pi^2$. In 2D rings ($\gamma = 0.5$), the energy difference is almost constant and the assumption of equal masses is well justified. Upon approaching the 1D limit, i.e., increasing γ, the amplitude of excitonic AB oscillations increases less for small m_e/m_h ratios but the effect is still revealed. As an example, in common III-V compound semiconductors the ratio of the electron and light-hole masses typically ranges from 0.6 to 0.9, and it can be seen in the inset of Fig. 3 that the reduction of the amplitude is small.

Figure 4 shows the AB oscillations of the exciton energy as a function of the magnetic flux Φ within one flux period at different values of γ and v_0. In agreement with Fig. 3, we find that the AB oscillations are retained for radius-to-width ratios ranging from $\gamma = 0.5$ to 10. This shows that the excitonic AB effect remains robust even in a ring of finite width. Upon increasing the γ values for different Φ values, we find mostly a moderate increase of the exciton energy, except in the vicinity of $\Phi = 0.5$ where even the reverse tendency can be observed.

In Fig. 5, we plot the amplitude of the excitonic AB oscillations for different interaction strength $v_0 = -1/\pi^2$, $-2/\pi^2$, $-3/\pi^2$ as γ is varied. We see that upon decreasing γ

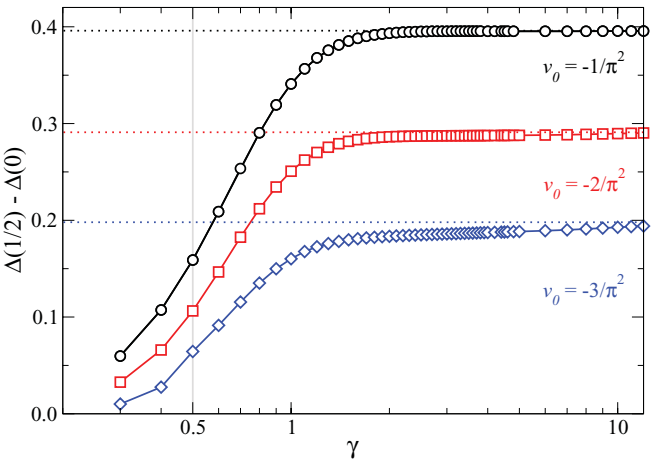

FIG. 5. (Color online) Amplitude of the AB oscillations $\Delta(1/2) - \Delta(0)$ as a function of radius-to-width ratio γ for different interaction strength v_0. The dashed horizontal lines correspond to the 1D limit,[14] the vertical line denotes the $\gamma = 0.5$ values.

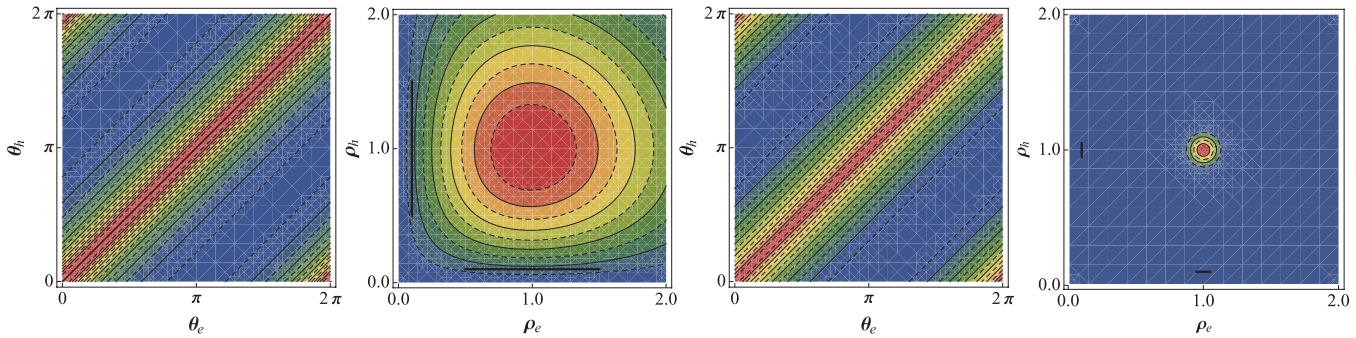

(a) $\gamma = 1$ (b) $\gamma = 1$ (c) $\gamma = 10$ (d) $\gamma = 10$

FIG. 6. (Color online) Dependence of the *local* wave-function probability $|\Psi|^2$ on (a,c) angular coordinates θ_e, θ_h and (b,d) radial coordinates $\rho_e = r_e/R$, $\rho_h = r_h/R$ for $\gamma = 1$ (a,b), and 10 (c,d) for $v_0 = -2/\pi^2$ and $\Phi = 0$. The values of $|\Psi(\theta_e,\theta_h)|^2$ and $|\Psi(\rho_e,\rho_h)|^2$ have been normalized to lie in $[0,1]$. The colors go from $|\Psi|^2 \in [0.9,1]$ (red) to $|\Psi|^2 \in [0,0.1]$ (blue) in steps of 0.05 for (a,c), 0.2 for (b) and 0.1 for (d). The thick black lines indicate in (b) and (d) the width W of the ring in each case.

from the nearly 1D behavior at $\gamma = 10$ toward $\gamma \approx 1.5$, there is only a slight decrease in the amplitude of the AB oscillations. Upon further decreasing γ, the oscillations weaken more rapidly, but even at $\gamma = 0.5$, they retain about 30–40% of their original value. Results for other values of v_0 are similar. This again shows that even for rather wide rings, the excitonic AB oscillations persist in this 2D case.

In Fig. 6, we show the exciton probablity density $|\Psi(\boldsymbol{r}_e,\boldsymbol{r}_h)|^2$ for different values of γ. We integrate $|\Psi|^2$ over the radial coordinates ρ_e and ρ_h and hence retain the angular dependence in Figs. 6(a) and 6(c), whereas in Figs. 6(b) and 6(d) we integrate out the angular degrees of freedom and retain the ρ_e-ρ_h dependence. From these figures, we conclude that the exciton fills the available width of the ring. Figures 6(a) and 6(c) show that the exciton is indeed bound, i.e., the majority of the weight of $|\Psi|^2$ resides along the diagonal $\theta_e = \theta_h$. Analogous results are obtained for different Φ and v_0. This is similar to the 1D behavior described in Refs. 14 and 20.

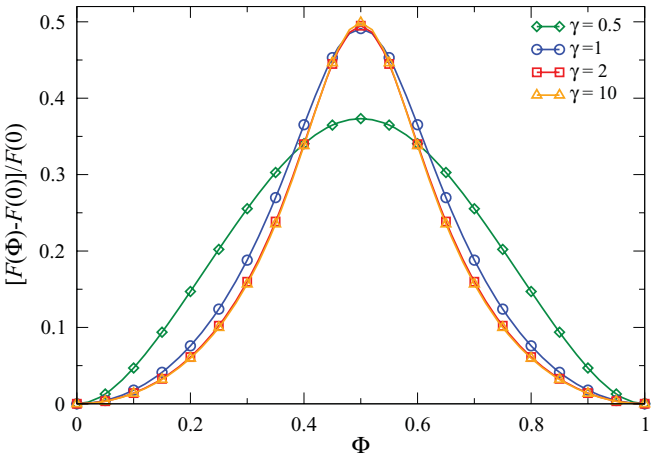

FIG. 7. (Color online) Normalized oscillator strength $[F(\Phi) - F(0)]/F(0)$ as a function of magnetic flux Φ for $\gamma = 0.5$, 1, 2, 5, and 10 at interaction strength $v_0 = -2/\pi^2$. Only every second data point is shown for clarity.

The oscillator strength, defined as

$$F = \frac{\left|\int d^2\boldsymbol{r}\,\Psi(\boldsymbol{r},\boldsymbol{r})\right|^2}{\int d^2\boldsymbol{r}_e \int d^2\boldsymbol{r}_h |\Psi(\boldsymbol{r}_e,\boldsymbol{r}_h)|^2}, \tag{12}$$

is plotted in Fig. 7. Large values of F correspond to a large transition matrix element from the exciton ground state into the vacuum. We find from Fig. 7 that the results for large γ are in good agreement with the 1D results.[14] And when decreasing the radius-to-width ratio γ, the value of F does not suddenly drop to zero, again emphasizing the robustness of the excitonic AB effect in a ring of finite width.

V. CONCLUSIONS

Our results suggest that the excitonic AB effect originally predicted for a 1D model[13,14] remains essentially unchanged when allowing for rings of finite widths as given by Eq. (2). We find that when we enlarge the ring width by one order of magnitude from $1/\gamma = 1/10$ to 1, the magnitude of the AB oscillations drops by about 15% only. In addition, we show that the qualitative behavior of the oscillations both for the spectral position as well as the oscillator strengths of the exciton luminescence lines are again governed by the relative strength of attractive Coulomb interaction to ring radius. Our results are in good agreement with recent experimental observations where the magnitude of the excitonic AB oscillations was observed to be about 0.5 meV at binding energies of 4.35 mV for rings of about 11–22 nm radius and $\gamma \approx 1$.[5] We also note that our confining potential (2) has been chosen to retain its *nonsimple connectedness* due to the infinitely repulsive centrifugal core at the center. Hence even for very wide rings, there is an essential difference with respect to the previously considered 2D confining potentials.[15,21,22,26–28] This demonstrates that it is not so much the width or the exact shape of the confining potential, but rather the avoidance of the ring center that is the important ingredient needed for the experimental observation of the excitonic AB effect.

Last, we expect that the effects of external electric fields[20,31,36] and the formation of charged excitons remain similarly robust in 2D, whereas disorder effects[24,37,38] should be less important than in the 1D case.

ACKNOWLEDGMENTS

We thank Andrea Fischer for valuable discussions and a critical reading of the manuscript. CGS is grateful to the Centre for Scientific Computing for hospitality and to Ministerio de Educación, Comunidad de Madrid, and the European Social Fund for funding the research stays at Warwick during which much of this work was done. Work at Madrid was supported by MICINN (projects Mosaico and MAT2010-17180).

*cglezsantander@fis.ucm.es

[1] A. Lorke, R. J. Luyken, M. Fricke, J. P. Kotthaus, G. Medeiros-Ribeiro, J. M. Garcia, and P. M. Petroff, Microelectron. Eng. **47**, 95 (1999).

[2] A. Lorke, R. J. Luyken, A. O. Govorov, J. P. Kotthaus, J. M. Garcia, and P. M. Petroff, Phys. Rev. Lett. **84**, 2223 (2000).

[3] R. J. Warburton, C. Schäflein, D. Haft, F. Bickel, A. Lorke, K. Karral, J. M. Garcia, W. Schoenfeld, and P. M. Petroff, Nature (London) **405**, 926 (2000).

[4] E. Ribeiro, A. O. Govorov, W. Carvalho, and G. Medeiros-Ribeiro, Phys. Rev. Lett. **92**, 126402 (2004).

[5] M. D. Teodoro, V. L. Campo, V. Lopez-Richard, E. Marega, G. E. Marques, Y. G. A. Gobato, F. Iikawa, M. J. S. P. Brasil, Z. Y. AbuWaar, V. G. Dorogan, Y. I. Mazur, M. Benamara, and G. J. Salamo, Phys. Rev. Lett. **104**, 086401 (2010).

[6] M. Bayer, O. Stern, P. Hawrylak, S. Safard, and A. Forchel, Nature (London) **405**, 923 (2000).

[7] M. Bayer, M. Korkusinski, P. Hawrylak, T. Gutbrod, M. Michel, and A. Forchel, Phys. Rev. Lett. **90**, 186801 (2003).

[8] F. Ding, N. Akopian, B. Li, U. Perinetti, A. Govorov, F. M. Peeters, C. C. Bof Bufon, C. Deneke, Y. H. Chen, A. Rastelli, O. G. Schmidt, and V. Zwiller, Phys. Rev. B **82**, 075309 (2010).

[9] W. Ehrenberg and R. E. Siday, Proc. Phys. Soc. Section B **62**, 8 (1949).

[10] Y. Aharonov and D. Bohm, Phys. Rev. **115**, 485 (1959).

[11] N. Byers and C. N. Yang, Phys. Rev. Lett. **7**, 46 (1961).

[12] T. Chakraborty and P. Pietiläinen, Solid State Commun. **87**, 809 (1993).

[13] A. Chaplik, Pis'ma Zh. Eksp. Teor. Fiz. **62**, 885 (1995) [JETP Lett. **62**, 900 (1995)].

[14] R. A. Römer and M. E. Raikh, Phys. Rev. B **62**, 7045 (2000).

[15] I. Galbrath, F. Braid, and R. Warburton, Phys. Status Solidi A **190**, 781 (2002).

[16] D. Haft, C. Schulhauser, A. Govorov, R. Warburton, K. Karrai, J. Garcia, W. Schoenfeld, and P. Petroff, Physica E **13**, 165 (2002).

[17] A. Govorov, A. Kalameitsev, R. Warburton, K. Karrai, and S. Ulloa, Physica E **13**, 297 (2002).

[18] K. Maschke, T. Meier, P. Thomas, and S. Koch, Eur. Phys. J. B **19**, 599 (2001).

[19] T. V. Shahbazyan, I. E. Perakis, and M. E. Raikh, Phys. Rev. Lett. **84**, 5896 (2000).

[20] A. M. Fischer, V. L. Campo, M. E. Portnoi, and R. A. Römer, Phys. Rev. Lett. **102**, 096405 (2009).

[21] H. Hu, D.-J. Li, J.-L. Zhu, and J.-J. Xiong, J. Phys. Condens. Matter **12**, 9145 (2001).

[22] H. Hu, J. L. Zhu, D. J. Li, and J. J. Xiong, Phys. Rev. B **63**, 195307 (2001).

[23] A. O. Govorov, S. E. Ulloa, K. Karrai, and R. J. Warburton, Phys. Rev. B **66**, 081309(R) (2002).

[24] L. G. G. V. Dias da Silva, S. E. Ulloa, and A. O. Govorov, Phys. Rev. B **70**, 155318 (2004).

[25] Z. Barticevic, M. Pacheco, J. Simonin, and C. R. Proetto, Phys. Rev. B **73**, 165311 (2006).

[26] J. Song and S. E. Ulloa, Phys. Rev. B **63**, 125302 (2001).

[27] M. Grochol, F. Grosse, and R. Zimmermann, Phys. Rev. B **74**, 115416 (2006).

[28] Z. Dai and J.-L. Zhu, J. Phys. Condens. Matter **19**, 346202 (2007).

[29] F. Palmero, J. Dorignac, J. C. Eilbeck, and R. A. Römer, Phys. Rev. B **72**, 075343 (2005).

[30] T. V. Bandos, A. Cantarero, and A. Garcia-Cristobal, Eur. Phys. J. B **53**, 99 (2006).

[31] B. Li and F. M. Peeters, Phys. Rev. B **83**, 115448 (2011).

[32] E. N. Bogachek and I. O. Kulik, Fiz. Nizk. Temp. **9**, 398 (1983) [Sov. J. Low Temp. Phys. **9**, 202 (1983)]; E. N. Bogachek and Uzi Q. Landman, Phys. Rev. B **52**, 14067 (1995); W.-C. Tan and J. C. Inkson, Semicond. Sci. Technol. **11**, 1635 (1996).

[33] V. M. Kovalev and A. V. Chaplik, Pis'ma Zh. Eksp. Teor. Fiz. **90**, 753 (2009) [JETP Lett. **90**, 679 (2009)].

[34] The vector potential is defined as usual such that $\oint \boldsymbol{A} \cdot d\boldsymbol{r} = \Phi h/e$.

[35] E. Lieb and W. Liniger, Phys. Rev. **130**, 1605 (1963).

[36] A. V. Maslov and D. S. Citrin, Phys. Rev. B **67**, 121304 (2003).

[37] T. Meier, P. Thomas, and S. Koch, Eur. Phys. J. B **22**, 249 (2001).

[38] P. Hui and Z. Jia-Lin, J. Phys. Condens. Matter **15**, 7287 (2003).